

Fischer–Tropsch Synthesis: Differences Observed in Local Atomic Structure and Selectivity with Pd Compared to Typical Promoters (Pt, Re, Ru) of Co/Al₂O₃ Catalysts

Gary Jacobs · Wenping Ma · Pei Gao ·
Branislav Todic · Tejas Bhatelia · Dragomir B. Bukur ·
Syed Khalid · Burtron H. Davis

Published online: 28 July 2012
© Springer Science+Business Media, LLC 2012

Abstract Pd was examined as a promoter for Fischer–Tropsch synthesis, and its effects on cobalt oxide reduction and product selectivities relative to commonly used promoters (i.e., Pt, Re, and Ru) at atomically equivalent levels were compared. Pd was identified to promote cobalt oxide reduction to even lower temperatures than Pt and Ru. However, Pd addition deleteriously affected product selectivity, and a clear shift to favor light products was observed. XANES analysis of an activated model catalyst revealed that Pd was in the reduced state. Local atomic structure was examined by EXAFS. Unlike Pt, Re, and Ru promoters, where previous investigations by groups such as Dr. Guzzi's and ours have only observed coordination of the promoter with cobalt, Pd displayed both direct coordination to Co as well as other Pd atoms. The results suggest that this feature may be responsible for the measurably higher light gas selectivities observed.

Keywords Fischer–Tropsch synthesis · Pd–Co/Al₂O₃ · Cobalt catalysts · Selectivity · Reduction promoters

1 Introduction

Fischer–Tropsch synthesis (FT) over cobalt catalysts is at the heart of current gas-to-liquids technology [1–4]. Active sites for FT on cobalt have been identified to be surface cobalt metal atoms [5]. To achieve high attrition resistance and adequate active site densities, γ -Al₂O₃ is commonly used as a support [6]. For standard air calcined catalysts, γ -Al₂O₃ displays strong interactions with cobalt oxides compared to less interacting supports, like SiO₂ [7, 8]. Thus, reduction promoters, such as Pt [7–10], Re [7, 11–13], and Ru [7, 14–16], are commonly added to facilitate the reduction of cobalt oxides in strong interaction with the support (e.g., TiO₂ and Al₂O₃). Cobalt surface site densities can thus be significantly improved so that cobalt is not wasted by remaining in the oxidized state—inactive for FT [7, 17].

In preliminary work at the Center for Applied Energy Research (CAER), Pd was identified as a very effective promoter of cobalt oxide reduction in Co/ γ -Al₂O₃ FT catalysts [18], as was observed previously by Dr. Guzzi's group for the selective hydrogenation of butadiene [19, 20].

However, if Pd is to be implemented, then it is important to determine whether it maintains high selectivity relative to the commonly used promoters at equivalent atomic levels. To maintain control, catalysts were synthesized from the same parent batch of cobalt nitrate on alumina. Stirred tank slurry reactors were used in order to obtain data relevant to a typical commercial slurry bubble column reactor. Selectivities are compared at equivalent conversion levels so that meaningful conclusions could be drawn.

The second aim of the work is to characterize Pd so that potential differences in reactivity and productivity might be explained in terms of structural differences relative to the promoters commonly used in FT. To that aim, we turned to the use of extended X-ray absorption fine structure

G. Jacobs · W. Ma · P. Gao · B. H. Davis (✉)
Center for Applied Energy Research, University of Kentucky,
2540 Research Park Drive, Lexington, KY 40511, USA
e-mail: burtron.davis@uky.edu

B. Todic · T. Bhatelia · D. B. Bukur
Department of Chemical Engineering, Texas A&M University at
Qatar, P.O. Box 23874, Doha, Qatar

S. Khalid
National Synchrotron Light Source, Brookhaven National
Laboratory, Brookhaven Ave., Upton, NY 11973, USA

spectroscopy (EXAFS). The application of this fruitful technique to the investigation of promoters of cobalt FT and CO hydrogenation catalysts was pioneered by Dr. Guzzi and his colleagues [10, 13, 21, 22], resulting in deeper understanding of catalyst structure at the local atomic level.

2 Experimental

The support used was Sasol Catalox-150 γ -Al₂O₃. It was first calcined at 400 °C in a muffle furnace for 4 h. A slurry impregnation method was performed, whereby the ratio of the volume of loading solution used to the weight of alumina was 1:1, such that approximately 2.5 times the pore volume of solution was used to prepare the catalyst in two steps [6]. Due to the solubility limit of cobalt [7], two impregnation steps were used. After each impregnation step, the catalyst was dried under vacuum in a rotary evaporator from 80 to 100 °C. This large batch of dried cobalt nitrate on alumina was split into several equivalent batches in order to add promoters. The promoters were added to be atomically equivalent to 0.5 % by weight Pt, and the precursors used were tetraammine palladium (II) nitrate, tetraammine platinum (II) nitrate, rhenium oxide (Re₂O₇), and ruthenium nitrosyl nitrate. The promoters were added dropwise to achieve incipient wetness impregnation. After final drying at 80–100 °C, the final catalysts were calcined at 350 °C under flowing air for 4 h. In order to ensure that an interaction was observed by EXAFS spectroscopy, a model catalyst having 1 % Pd by weight was also prepared.

2.1 BET Measurements

BET measurements for the catalysts were conducted using a Micromeritics Tri-Star system to determine the loss of surface area with loading of the metal. Prior to the measurement, samples were slowly ramped to 160 °C and evacuated for 24 h to approximately 50 m Torr.

2.2 Temperature Programmed Reduction (TPR)

Temperature programmed reduction (TPR) profiles of fresh catalyst samples were obtained using a Zeton Altamira AMI-200 unit. Calcined fresh samples were first heated and purged in flowing argon to remove traces of water. TPR was performed using 30 cm³/min of a 10 % H₂/Ar mixture referenced to argon. The ramp rate was 5 °C/min from 50 to >1,000 °C.

2.3 Hydrogen Chemisorption with Pulse Reoxidation

Hydrogen chemisorption measurements were performed using a Zeton Altamira AMI-200 unit, which utilizes a thermal conductivity detector (TCD). The sample weight was always ~0.220 g. The catalyst was activated at 350 °C for 10 h using a flow of pure hydrogen and then cooled under flowing hydrogen to 100 °C. The sample was then held at 100 °C under flowing argon to prevent physisorption of weakly bound species prior to increasing the temperature slowly to the activation temperature. At that temperature, the catalyst was held under flowing argon to desorb the remaining chemisorbed hydrogen so that the TCD signal returned to the baseline. The TPD spectrum was integrated and the number of moles of desorbed hydrogen determined by comparing to the areas of calibrated hydrogen pulses. Prior to experiments, the sample loop was calibrated with pulses of nitrogen in helium flow and compared against a calibration line produced from gas tight syringe injections of nitrogen under helium flow. A H:Co ratio of 1:1 was assumed, as determined by Reuel and Bartholomew [23].

After TPD of hydrogen, the sample was reoxidized at the activation temperature by injecting pulses of pure oxygen in helium referenced to helium gas. After oxidation of the cobalt metal clusters, the number of moles of oxygen consumed was determined, and the percentage reduction calculated assuming that the Co⁰ reoxidized to Co₃O₄. While the uncorrected dispersions (uc) are based on the assumption of complete reduction, the corrected dispersions (c), which are reported in this work, include the percentage of reduced cobalt [7, 17] as follows.

$$\%D_{\text{uncorrected}} = \frac{(\# \text{ of Co}^0 \text{ atoms on surface} \times 100 \%) / (\text{total} \# \text{ Co atoms})}{100}$$

$$\%D_{\text{corrected}} = \frac{(\# \text{ of Co}^0 \text{ atoms on surface} \times 100 \%) / [(\text{total} \# \text{ Co atoms}) (\text{fraction reduced})]}{100}$$

2.4 In situ EXAFS/XANES Spectroscopies

EXAFS/XANES spectra were recorded in transmission mode near the Pd K-edge at the National Synchrotron Light Source (NSLS) at Brookhaven National Laboratory, Upton, New York, Beamline X18-b. The beamline was equipped with a Si (111) channel-cut monochromator. A crystal detuning procedure was used to help remove harmonic content from the beam and make the relative response of the incident and transmission detectors more linear. The X-ray flux for the beamline was on the order of 1 E 10 photons per second at 100 mA and 2.8 GeV, and the usable energy range at X-18b is from 5.8 to 40 keV. EXAFS

spectra were recorded near the boiling temperature of liquid nitrogen to minimize contributions to the dynamic Debye–Waller factor. A sample thickness was determined by calculating the amount in grams per square centimeter of sample, w_D , by utilizing the thickness equation:

$$w_D = \ln(I_0/I_t) / \sum \left\{ (m/r)_j w_j \right\}$$

where m/r is the total cross section (absorption coefficient/density) of element j in the sample at the absorption edge of the EXAFS element under study in cm^2/g , w_j is the weight fraction of element j in the sample, and $\ln(I_0/I_t)$ was taken over a typical range of 1–2.5. An average value of w_D from inputting both values was employed. Based on the calculation for w_D , and the cross-sectional area of the pellet, the grams were calculated. The catalysts were prepared in the same manner as a reaction test. However, following the H_2 -posttreatment step, the catalyst was cooled down and solidified in the startup Polywax. Samples were cut and pressed to make self-supporting wafers. EXAFS data reduction and fitting were carried out using the WinXAS program [24], Atoms [25], FEFF [26], and FEFFIT [27] programs. The k - and r -ranges were chosen to be approximately $2.5\text{--}12.75 \text{ \AA}^{-1}$ and $1.8\text{--}2.8 \text{ \AA}$, respectively. XANES spectra were compared qualitatively following normalization.

2.5 Catalyst Testing

Typically, the catalyst (15 g) was ground and sieved to 170–325 mesh before loading into a fixed-bed reactor for 15 h of *ex situ* reduction at 350 °C and atmospheric pressure using a gas mixture of H_2/He with a molar ratio of 1:3. The reduced catalyst was then transferred to a 1-L continuously stirred tank reactor (CSTR) which was previously charged with 315 g of melted Polywax 3000, under the protection of a N_2 inert gas. The transferred catalyst was further reduced *in situ* at 230 °C at atmospheric pressure using pure hydrogen for another 10 h before starting the FT reaction. In this study, the FT conditions were 220 °C, 2.2 MPa, $\text{H}_2/\text{CO} = 2.1$. The space velocity varied between 3.0 and 13 NL/g-cat/h. in order to give about 50 % CO conversion in different tests. This allows us to compare the differences in hydrocarbon selectivity data resulting from the promoter effect, without variations in reaction conditions.

3 Results and Discussion

Weight percentages of promoters and cobalt are listed in the first column of Table 1. Porosity data are also provided, and indicate that there is a noticeable difference in specific surface area following loading of the metal components.

Table 1 Results of BET surface area and porosity measurements

Description	BET surface area (m^2/g)	Average pore volume (cm^3/g)	Average pore diameter (nm)
Catalox-150 $\gamma\text{-Al}_2\text{O}_3$	140	0.44	10.2
25 % Co/ $\gamma\text{-Al}_2\text{O}_3$	99	0.27	11.1
0.27 % Pd–25 % Co/ $\gamma\text{-Al}_2\text{O}_3$	104	0.27	10.4
0.50 % Pt–25 % Co/ $\gamma\text{-Al}_2\text{O}_3$	102	0.27	10.4
0.26 % Ru–25 % Co/ $\gamma\text{-Al}_2\text{O}_3$	106	0.27	10.0
0.48 % Re–25 % Co/ $\gamma\text{-Al}_2\text{O}_3$	106	0.26	9.7

In reproducibility tests, measured variations were <2.0 % for BET and average pore volume parameters, and <0.2 % for average pore diameters

However, if the main contributor to the support is alumina, then the surface areas of what the catalysts should be, assuming no pore blocking, can be estimated. A weight percentage loading of 25 % Co is equivalent to roughly 33 % by weight Co_3O_4 . If alumina solely contributes to surface area, then the area of the cobalt catalysts—neglecting the promoter—should be $0.67 \times 150 \text{ m}^2/\text{g}$ (nominal) = $\sim 100 \text{ m}^2/\text{g}$. None of the catalysts exhibited areas that were, within experimental error, below this value. Therefore, significant pore blocking of the catalysts did not occur. Moreover, the average pore diameter was consistent with the value obtained by measuring the support.

The first characterization technique to measure the effectiveness of the different promoters was TPR [28], and results are summarized in Fig. 1. The unpromoted 25 % Co/ $\gamma\text{-Al}_2\text{O}_3$ catalyst displayed a number of different features. Cobalt oxide (Co_3O_4) and cobalt aluminate are present once a cobalt alumina catalyst is calcined in air, and higher loadings favor Co_3O_4 as being the primary species present [8, 29, 30]. In agreement with earlier XRD studies as a function of temperature [30], as well as standard TPR investigations [7, 31], TPR EXAFS-XANES experiments have confirmed that the latter species reduce at very high temperatures (>800 °C), while the former reduces in two steps [8]: $\text{Co}_3\text{O}_4 + \text{H}_2 = 3\text{CoO} + \text{H}_2\text{O}$ and $\text{CoO} + \text{H}_2 = \text{Co}^0 + \text{H}_2\text{O}$. The second step consumes three times as much hydrogen as the first step. The first reduction step occurs between 300 and 350 °C. A low temperature shoulder may indicate the decomposition of some residual cobalt nitrate. The CoO, however, interacts strongly with alumina and reduces to the metal over a broad temperature range leading up to about 750 °C. There is also a fraction of larger particles, in weak interaction with the support, that reduce as a high temperature

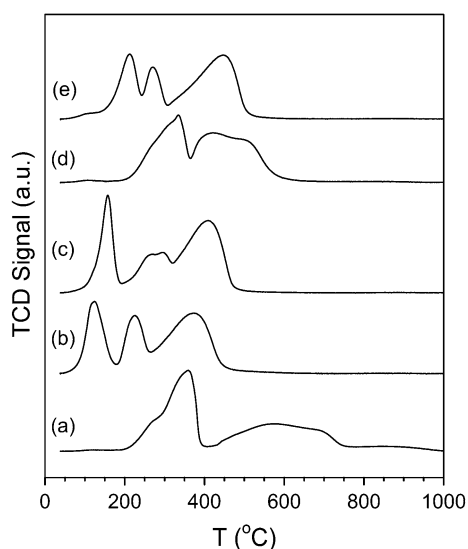


Fig. 1 TPR profiles of, moving upward **a** 25 % Co/ γ -Al₂O₃; **b** 0.273 % Pd–25 % Co/ γ -Al₂O₃; **c** 0.5 % Pt–25 % Co/ γ -Al₂O₃; **d** 0.477 % Re–25 % Co/ γ -Al₂O₃; **e** 0.259 % Ru–25 % Co/ γ -Al₂O₃

shoulder in the Co₃O₄ to CoO reduction peak [7]. A similar two-step reduction process was also observed by in situ EXAFS and XRD investigations over silica supported cobalt catalysts [32, 33] and smaller, more strongly interacting species, have been observed to reduce only at higher temperatures [34]. Upon addition of the different reduction promoters (e.g., Pt [7–10], Re [7, 11–13], Ru [7, 14–16], and Pd [18–20]), reduction of cobalt oxides is facilitated, and a separation occurs in the peak for larger CoO crystallites from that of Co₃O₄ to CoO, as well as separation from the peak for reduction of smaller CoO crystallites in strong interaction with the support. As noted in our earlier investigation [7], Re oxide reduces at about the same temperature as Co₃O₄ reduction to CoO, and since metallic Re is needed to facilitate reduction—perhaps by a H₂ dissociation and spillover mechanism—only the high temperature step of CoO to Co⁰ (i.e., the one that generates the active sites for FT) is promoted.

TPR profiles only provide a qualitative measure of reduction. To better quantify the extent of reduction and, more importantly, assess active site densities, hydrogen chemisorption [23, 35, 36] with pulse reoxidation [7, 17] was carried out, and the results are reported in Table 2. The H₂ desorbed per gram of catalyst values provide a direct correlation with the number of available surface Co⁰ sites following activation, and reveal a significant increase with addition of the common reduction promoters (i.e., Pt, Re, Ru), as well as Pd. By taking into account the extent of reduction, as measured by oxygen titration, the corrected values for particle size show that there was a measurable decrease in particle size. This can be correlated with the TPR profiles. Recall that a heterogeneous distribution of sites is suggested by the TPR profiles, with larger CoO particles reducing as a sharp feature in the tail end of Co₃O₄ to CoO reduction, whereas the smaller particles in stronger interaction with the support reduce in the broad feature up to about 750 °C. With a standard hydrogen activation treatment of the unpromoted 25 % Co/ γ -Al₂O₃ catalyst, the larger CoO crystallites will undergo reduction, while a relatively smaller fraction of the strongly interacting cobalt oxide species with the support (i.e., smaller species) will reduce. By adding the reduction promoters, a significantly greater fraction of the CoO crystallites in close interaction with the support are reduced, and thus, the average Co⁰ cluster size decreases. Moreover, these smaller crystallites provide a greater fraction of cobalt atoms exposed to the surface, significantly improving the overall cobalt active site density.

In the past, Dr. Guzzi's group [10, 13, 21, 22] and others [15, 37–40] have evaluated certain promoters to establish whether or not direct contact could be observed using the EXAFS technique. Pt [10, 39], Re [13, 37, 38], and Ru [15, 40] have all been evaluated. The promoting impact of Pd on cobalt reduction was investigated by Dr. Guzzi's group for Pd–Co/Al₂O₃ catalysts used in the selective hydrogenation of 1,3-butadiene [19, 20]. In this case, we are

Table 2 Results of hydrogen chemisorption/pulse reoxidation after activation in hydrogen at 350 °C for 10 h

Sample description	H ₂ desorbed per g catalyst	Uncorrected % dispersion	Uncorrected cobalt cluster size (nm)	O ₂ uptake per g catalyst	% reduction	Corrected % dispersion	Corrected cobalt cluster size (nm)
25 % Co/ γ -Al ₂ O ₃	64	3.0	34	1,540	55	5.5	19
0.27 % Pd–25 % Co/ γ -Al ₂ O ₃	125	5.9	18	2,040	72	8.1	13
0.50 % Pt–25 % Co/ γ -Al ₂ O ₃	120	5.7	18	1,930	68	8.3	12
0.26 % Ru–25 % Co/ γ -Al ₂ O ₃	139	6.6	16	2,000	71	9.3	11
0.48 % Re–25 % Co/ γ -Al ₂ O ₃	143	6.8	15	1,900	67	10.1	10

In reproducibility tests, measured variations in H₂ desorption and O₂ titration parameters were <1.0 %

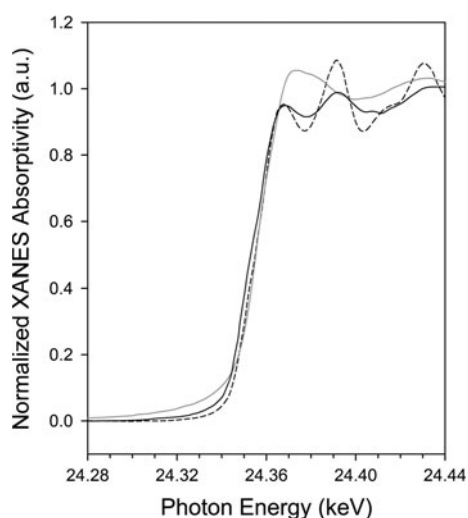


Fig. 2 XANES spectra at the Pd K-edge for (solid black line) 1 % Pd–25 % Co/ γ -Al₂O₃; (dashed line) Pd⁰ foil; and (solid gray line) PdO reference

evaluating its effectiveness as a promoter for FT synthesis, requiring the need for an examination of local interactions at the atomic level. XANES results at the Pd K-edge are provided in Fig. 2 and compare the activated 1 % Pd to 25 % Co/ γ -Al₂O₃ catalyst with reference compounds. By comparing the white line intensity of the Pd in the catalyst with those of Pd⁰ and PdO, it is evident that the Pd, following activation, exists in the metallic state. This is in direct line with the other promoters examined previously.

The question of local atomic structure can be probed by EXAFS spectroscopy. Previously, it was observed with Pt [10, 39], Re [13, 38], and Ru [40] that in many cases each promoter was coordinated solely to Co and no evidence of a promoter–promoter (e.g., Pt–Pt, etc.) interaction was identified. In the case of Pd, Fig. 3 shows a comparison of the Fourier transform magnitudes. The maximum in the first Pd coordination shell peaks at a distance significantly shorter than that of Pd–Pd coordination. Moreover, the higher coordination shells are also very obviously at lower coordination distances than observed with the Pd metal foil. The phase uncorrected distance of the first coordination shell matches well with what is to be expected for a Pd–Co interaction. What is structurally different about Pd relative to the other promoters previously examined is that the first shell coordination peak exhibits considerable asymmetric character, suggesting the possibility of another atomic interaction. The distance of this feature does match with that of the first shell of Pd–Pd coordination in the foil. Qualitatively, it appears that there is Pd that is coordinated to Co particles and this coordination extends to higher shells, suggesting either that Pd is on the surface of the particle (e.g., in line with a H₂ dissociation and spillover mechanism [12]) or embedded within the particle (e.g.,

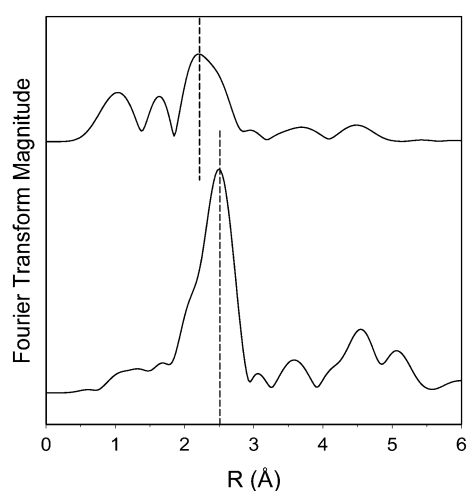


Fig. 3 k^2 -weighted EXAFS Fourier transform magnitude spectra of (top) 1 % Pd/25 % Co/ γ -Al₂O₃ and (bottom) Pd⁰ foil reference

mixing/alloying [15, 41], and with it the possibility of a chemical promotion). The presence of Pd–Pd coordination may indicate some isolated particles of Pd with ultra-high dispersion, since Pd–Pd coordination is not observed in higher shells, or that Pd in surface contact with Co exists as multiple atoms (e.g., ultra-highly dispersed islands).

Fittings for both Pd in the catalyst and Pd metal foil were carried out using the atoms [25], FEFF [26], and FEFFIT [27] programs, and results are reported in Fig. 4 and Table 3. The fitting of the foil was excellent by assuming that the amplitude reduction factor, S_0^2 , was 0.90 and therefore, we used this value in the fitting of the catalyst as well. The e_0 shift and σ^2 Debye–Waller values were reasonable for the cases where good fittings were obtained, but these parameters are excluded from the table for the sake of brevity. Three fittings were attempted for the catalyst. By considering only Pd–Co interaction, the fittings fails, as the r -factor is far too large, at 18.1 %. Likewise, including only a Pd–Pd interaction also yields unsatisfactory results, and the r -factor is too large, at 11.5 %. However, including both the Pd–Co and Pd–Pd interactions, as suggested from the qualitative explanation, does yield a satisfying fitting, with the r -factor dropping to about 0.2 %. The low coordination numbers are indicative of very highly dispersed Pd according to one of the scenarios previously described.

Note that the different catalysts experienced different initial deactivation patterns. In this work, adjusting the space velocity to the 50 % conversion level was made only after a period of relative pseudo-stability was achieved. We anticipate that a more comprehensive manuscript detailing the effect of promoter type on initial activity, stability, and selectivity will be completed in the near future. With these considerations in mind, Table 4 summarizes the impact of Pd promoter on the FT activity and selectivity of Co/Al₂O₃

Fig. 4 EXAFS fittings on data recorded near the Pd K-edge, including (left) raw k^2 -weighted $\chi(k)$ versus k data; (middle) (solid line) filtered k^2 -weighted $\chi(k)$ versus k data and (filled circles) result of the fitting; and (right) (solid line) raw k^2 -weighted Fourier transform magnitude spectra and (filled circles) result of the fitting for **a** 1 % Pd–25 % Co/ γ -Al₂O₃ and **b** Pd⁰ foil

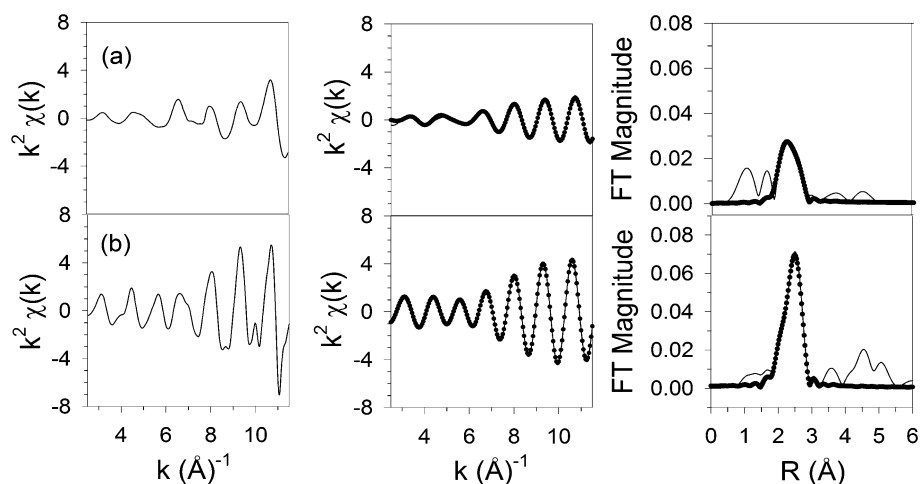


Table 3 Coordination number and distance calculated from EXAFS fitting

Sample description	N Pd–Co metal	R Pd–Co metal (Å)	N Pd–Pd metal	R Pd–Pd metal (Å)	r-factor
Pd ⁰ foil	–	–	12.0*	2.737 (0.0027)	0.00349
1.0 % Pd–25 % Co/Al ₂ O ₃ fitting with Pd–Co only	3.7 (1.1)	2.587 (0.0316)	–	–	0.181
1.0 % Pd–25 % Co/Al ₂ O ₃ fitting with Pd–Pd only	–	–	3.4 (2.2)	2.702 (0.0202)	0.115
1.0 % Pd–25 % Co/Al ₂ O ₃ fitting with Pd–Co and Pd–Pd	2.2 (1.3)	2.594 (0.0155)	2.2 (0.74)	2.711 (0.0077)	0.00186

The fitting ranges were $\Delta k = 2.5$ – 12.75 \AA^{-1} and $\Delta R = 1.85$ – 2.85 \AA . $S_0^2 = 0.9$

* Fixed parameter

Table 4 Effect of Re, Pt, Pd, and Ru promoters on the activity and hydrocarbon selectivity of 25 % Co/Al₂O₃ catalyst

Catalyst	TOS (h)	Space velocity NI/g-cat/h	CO conversion, %	Selectivity (carbon atom %)		
				CH ₄	C ₂ –C ₄	C ₅ +
25 % Co/Al ₂ O ₃	58–73	4.3	49.4	7.9	8.8	83.4
0.48 % Re–25 % Co/Al ₂ O ₃	44–68	8.0	49.6	7.2	6.9	86.0
0.5 % Pt–25 % Co/Al ₂ O ₃	46–68	5.6	48.0	8.3	8.8	83.0
0.27 % Pd–25 % Co/Al ₂ O ₃	51–73	4.9 ^a	50.3	11.5	12.6	75.9
0.26 % Ru–25 % Co/Al ₂ O ₃	51–81	7.6	51.3	7.0	6.2	86.8

^a Note that the catalyst was quite deactivated by this point. More recent results taken at the onset prior to deactivation show similar selectivities, but the space velocities were higher: 8 for the Pd catalyst, but 13 for the common promoters (Pt, Re, Ru)

Other reaction conditions: 220 °C, 300 psig, H₂/CO = 2.1

CO₂ selectivity was 0.35–0.75 %

Note that weight percentages are given and that equivalent atomic amounts of promoter were used

catalysts relative to common promoters (i.e., Pt, Re, Ru), as well as the case of the unpromoted catalyst. Note that a significantly lower space velocity was required to achieve ~50 % conversion in the case of the Pd promoted catalyst. This indicates that Pd–Co/Al₂O₃ is not as effective at turning over CO as compared to the Co/Al₂O₃ catalysts containing the typical promoters. Addition of Pd increases the light product selectivity significantly, with a 3.2–4.5 % increase in methane, a 3.8–6.4 % increase in C₂–C₄ selectivities, and a decrease in C₅+

7.1–10.9 % over the other catalysts tested. We attribute this excessive hydrogenation activity to the presence of clusters of promoter atoms with Pd, which were not observed in the cases of Pt, Re, and Ru. Because the catalysts were prepared in the same manner, the results suggest that Pd has a propensity to form these islands or clusters.

One should also consider the possibility that there may be less island formation at the lower loading of 0.27 % Pd. In that case, greater H₂ solubility might contribute to the adverse selectivities observed. However, it should be noted

that internal olefin selectivity is generally not observed to be sensitive to $P(H_2)$ [42]. We observed a significant increase in internal olefin selectivity from 14 % for the unpromoted catalyst to 27 % with the Pd promoted catalyst. Therefore, the results suggest that another factor is responsible for the differences in selectivity, and the proposal that a fraction of Pd is present as separate islands is consistent with this observation.

4 Conclusions

In some respects, Pd behaves similarly to the typical promoters used (i.e., Pt, Re, and Ru) in Co/Al₂O₃ FT catalysts. It acts as a reduction promoter, significantly increasing the number of active sites following activation. Like the other promoters, XANES revealed that Pd exists in the metallic state. However, unlike the other promoters, where only promoter–cobalt atomic interactions were observed at low promoter concentration levels, both Pd–Co and Pd–Pd coordination were observed in EXAFS spectroscopy. Islands of Pd on cobalt or isolated Pd clusters were likely responsible for the higher C₁ and other light gas selectivities observed, and for the 7–11 % drop in C₅+ selectivity measured relative to the typical promoters used (or unpromoted case). The selectivities were recorded at the same conversion level of ~50 % after a period of relative stability was achieved. Because a significantly lower space velocity was needed to provide the 50 % conversion level in the case of Pd–Co/Al₂O₃, the catalyst was not as effective at turning over CO relative to the Co/Al₂O₃ catalysts containing typical promoters (i.e., Pt, Re, Ru).

Acknowledgments We thank the Qatar National Research Fund (Grant #NPRP 08-173-2-050) and the Commonwealth of Kentucky for financial support. We would also like to thank Dr. Nebojsa Marinkovic for his assistance at Beamline X-18b. Use of the National Synchrotron Light Source, Brookhaven National Laboratory, was supported by the U.S. Department of Energy, Office of Science, Office of Basic Energy Sciences, under Contract No. DE-AC02-98CH10886.

References

- van Berge PJ, Barradas S, van de Loosdrecht J, Visagie JL (2001) Erdol Erdgas Kohle 117:138
- Steynberg AP, Dry ME (eds) (2004) Fischer–Tropsch technology, 1st edn, Stud Surf Sci Catal, Vol 152. Elsevier Science, Amsterdam, The Netherlands
- Davis BH, Occelli ML (eds) (2007) Fischer–Tropsch synthesis, catalysts and catalysis, Stud Surf Sci Catal, Vol 163. Elsevier Science, Amsterdam, The Netherlands
- Davis BH, Occelli ML (eds) (2009) Advances in Fischer–Tropsch synthesis, catalysts and catalysis. CRC Press, Taylor & Francis Group, Boca Raton, FL
- Iglesia E (1997) Appl Catal A Gen 161:59
- Espinoza RL, Visagie JL, van Berge PJ, Bolder FH (1998) Sas-tech Limited, US Patent 5,733,839
- Jacobs G, Das TK, Zhang YQ, Li JL, Racoillet G, Davis BH (2002) Appl Catal A Gen 233:263
- Jacobs G, Ji Y, Davis BH, Cronauer DC, Kropf AJ, Marshall CL (2007) Appl Catal A Gen 333:177
- Schanke D, Vada S, Blekkan EA, Hilmen AM, Hoff A, Holmen A (1995) J Catal 156:85
- Guczi L, Bazin D, Kovacs I, Borko L, Schay Z, Lynch J, Parent P, Lafon C, Stefler Gy, Koppány Zs, Sajo I (2002) Top Catal 20:129
- Hilmen AM, Schanke D, Holmen A (1996) Catal Lett 34:143
- Hilmen AM, Schanke D, Holmen A (1996) Catal Lett 38:143
- Bazin D, Borko L, Koppány Zs, Kovacs I, Stefler Gy, Sajo LI, Schay Z, Gucci L (2002) Catal Lett 84:169
- Kogelbauer A, Goodwin JG Jr, Oukaci R (1996) J Catal 160:125
- Iglesia E, Soled SL, Fiato RA, Via GH (1993) J Catal 143:345
- Guczi L, Sundararajan R, Koppány Zs, Zsoldos Z, Schay Z, Mizukami F, Niwa S (1997) J Catal 167:482
- Vada S, Hoff A, Adnanes E, Schanke D, Holmen A (1995) Top Catal 2:155
- Ribeiro MC (P.T.A. Sumodjo advisor and B.H. Davis internship advisor) (2009), PhD thesis, Instituto de Química, Universidade de São Paulo
- Sarkany A, Zsoldos Z, Stefler Gy, Hightower JW, Gucci L (1995) J Catal 157:179
- Sarkany A, Zsoldos Z, Stefler Gy, Hightower JW, Gucci L (1994) Science and technology in catalysis. Stud Surf Sci Catal 92:99
- Bazin D, Kovacs I, Lynch J, Gucci L (2003) Appl Catal A Gen 242:179
- Bazin D, Gucci L (2004) Natural gas conversion VII. Stud Surf Sci Catal 147:343
- Reuel RC, Bartholomew CH (1984) J Catal 85:63
- Ressler T (1998) J Synchrotron Rad 5:118
- Ravel B (2001) J Synchrotron Rad 8:314
- Rehr JJ, Albers RC (2000) Rev Mod Phys 72:621
- Newville M, Ravel B, Haskel D, Stern EA, Yacoby Y (2005) Phys B 208–209:154
- Arnoldy P, Moulijn JA (1985) J Catal 93:38
- Wang W-J, Chen Y-W (1991) Appl Catal 77:223
- Bechara R, Balloy D, Dauphin J-Y, Grimblot J (1999) Chem Mater 11:1703
- Sexton BA, Hughes AE, Turney TW (1986) J Catal 97:390–406
- Khodakov AY, Lynch J, Bazin D, Rebours B, Zanier N, Moisson B, Chaumette P (1997) J Catal 168:16
- Jacobs G, Ma W, Davis BH, Cronauer DC, Kropf AJ, Marshall CL (2010) Catal Lett 140:106
- Sietsma JRA, den Breejen JP, de Jongh PE, van Dillen AJ, Bitter JH, de Jong KP (2007) Stud Surf Sci Catal 167:55
- Jones RD, Bartholomew CH (1988) Appl Catal 39:77
- Bartholomew CH (1990) Catal Lett 7:27
- Ronning M, Nicholson DG, Holmen A (2001) Catal Lett 72:141
- Jacobs G, Chaney JA, Patterson PM, Das TK, Davis BH (2004) Appl Catal A Gen 264:203
- Jacobs G, Chaney JA, Patterson PM, Das TK, Maillot JC, Davis BH (2004) J Synchrotron Rad 11:414
- Ma W, Jacobs G, Ji Y, Bhatelia T, Bukur DB, Khalid S, Davis BH (2011) Top Catal 54:757
- Tsubaki N, Sun S, Fujimoto K (2001) J Catal 199:236
- Herzog K, Gaube J (1989) J Catal 115:337